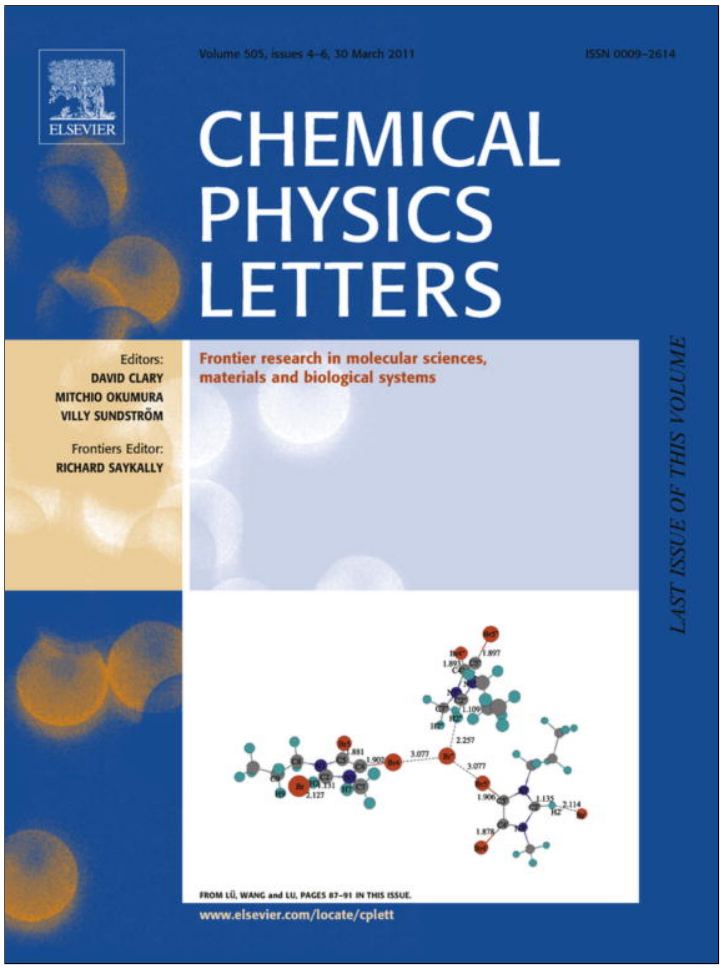

Chemical Physics Letters 505 (2011) 106–111

Contents lists available at ScienceDirect

Chemical Physics Letters

journal homepage: www.elsevier.com/locate/cplett

Highly efficient electron-stimulated desorption of benzene from amorphous solid water ice

J.D. Thrower [a,*], M.P. Collings [a], F.J.M. Rutten [b], M.R.S. McCoustra [a,*]

[a] School of Engineering and Physical Sciences, Heriot-Watt University, Edinburgh EH14 4AS, UK
[b] School of Pharmacy and iEPSAM, Keele University, Keele ST5 5BG, UK

ARTICLE INFO

Article history:
Received 22 October 2010
In final form 13 February 2011
Available online 16 February 2011

ABSTRACT

The desorption of benzene (C_6H_6) from the surface of compact amorphous solid water (ASW) during irradiation with electrons in the range 100–350 eV has been investigated. Two desorption components, with particularly large cross-sections, were present in the observed desorption signal. The fast component, with a cross-section of $> 10^{-15}$ cm^2, is attributed to desorption of isolated C_6H_6 molecules that are π-hydrogen bonded to small clusters of water (H_2O) molecules on the compact ASW surface. The slower component, with a cross-section of *ca.* 10^{-16} cm^2, is attributed to a more complex desorption process involving larger C_6H_6 islands on the compact ASW surface. Possible desorption mechanisms are discussed.

1. Introduction

The low energy electron irradiation of condensed matter is of interest in a wide range of fields. In astrophysics, for example, interstellar and planetary ices are exposed to a continuous bombardment of energetic particles, including both low and high energy electrons. The interaction of cosmic ray particles with interstellar and solar system ices results in a cascade of secondary electrons, which provide an important energy input to promote chemical change [1,2]. The interaction of low energy electrons with biological systems has also been investigated. The passage of high energy radiation such as X-rays in routine medical procedures results in the formation of secondary electrons which may go on to interact with DNA and other important biomolecules [3].

Water plays an important role in a diverse range of systems, including astrophysical and biological environments. The interaction of low energy electrons with condensed H_2O has therefore been the subject of intense research effort. The low energy electron-stimulated desorption (ESD) of neutral and ionic species from adsorbed layers of H_2O has been investigated in detail over recent years. The desorption of anionic H^- species from amorphous solid water (ASW) was shown to have a low threshold of *ca.* 5 eV, attributed to a dissociative electron attachment (DEA) mechanism [4]. Desorption of H_2 was also observed [5], with Frenkel-type excitons being implicated in the process for electron energies < 11 eV, whilst the recombination of cationic species formed in the ice with quasi-free or trapped electrons is thought to be responsible for H_2 desorption at higher electron energies. The desorption of neutral atomic species [6], formation of O_2 [7] and sputtering of intact H_2O molecules have also been observed [8], whilst the morphology of the H_2O film has been shown to influence electron stimulated processes [9]. Irradiation at higher energies (5 keV) has revealed the formation of H_2, O_2 and H_2O_2 which remain trapped within the ice matrix until subsequent thermal desorption [10].

In this letter, we report the highly efficient desorption of isolated C_6H_6 molecules adsorbed on the top of a compact (non-porous) ASW film. We derive a desorption cross-section in excess of 10^{-15} cm^2. We highlight that, for the electron energy range investigated, the measured large cross-section is consistent with the generation of a cascade of secondary electrons within the compact ASW film. We discuss possible mechanisms for the observed C_6H_6 desorption and suggest that exciton-driven energy transfer from the bulk compact ASW to the surface region may play an important role. This efficient C_6H_6 desorption observed in the presence of compact ASW is in marked contrast to the irradiation of C_6H_6 multilayers and a monolayer of C_6H_6 adsorbed on an amorphous SiO_2 substrate, where no C_6H_6 ESD is observed. X-ray photoelectron spectroscopy (XPS) revealed the build-up of a carbonaceous deposit after repeated electron irradiation experiments. This is constent with previous studies showing that the irradiation of C_6H_6 films primarily results in dehydrogenation.

2. Experimental

The experiments were performed in an ultrahigh vacuum (UHV) chamber with a base pressure of $< 2 \times 10^{-10}$ Torr [11,12]. The substrate used in these experiments was a polished stainless steel disc

* Corresponding authors. Present address: Department of Physics and Astronomy, Aarhus University, 8000 Aarhus C, Denmark (J.D. Thrower). Tel.: +45 89423629.
E-mail addresses: thrower@phys.au.dk (J.D. Thrower), m.r.s.mccoustra@hw.ac.uk (M.R.S. McCoustra).

0009-2614/$ - see front matter © 2011 Elsevier B.V. All rights reserved.
doi:10.1016/j.cplett.2011.02.029

coated with a thin (*ca.* 200 nm) film of amorphous SiO_2 which has been developed for use as a grain mimic for investigations of the interstellar gas–grain interaction [12]. The substrate was held at a temperature of 115 ± 2 K throughout. Electron irradiation experiments were performed with C_6H_6 adsorbed on both this substrate and a thick (*ca.* 10^2 layers) H_2O film deposited upon the SiO_2 using an effusive molecular beam under conditions known to result in the formation of compact ASW [13]. This film therefore contains little internal porosity, in contrast to ASW deposited at temperatures below *ca.* 80 K using background deposition. C_6H_6 exposures of 1 and 10 L (1 L = 10^{-6} Torr s) were used in the majority of the experiments described here. Previous experiments [14] indicate that these exposures result in the formation of sub-monolayer films of C_6H_6 on compact ASW, with larger extended islands of C_6H_6 being present at the higher exposure. The films were irradiated with an electron beam with a flux of *ca.* 1×10^{14} e^- cm^{-2} s^{-1} such that beam-induced substrate heating and surface charging are avoided [15]. Beam flux measurements were made by measuring the electron current through the sample. No significant difference was observed between flux measurements made on the SiO_2 and uncoated side of the substrate. Desorbing C_6H_6 molecules were detected using a differentially pumped pulse counting quadrupole mass spectrometer (QMS) with a well-defined line-of-sight to the substrate. The configuration of the QMS meant that only desorbing neutral species could be detected. De-ionised H_2O and spectroscopy grade C_6H_6 (Fluka) were further purified using repeated freeze–pump–thaw cycles on independent high vacuum manifolds to avoid cross-contamination. X-ray photoelectron spectroscopy (XPS) measurements were carried out at the University of Nottingham, UK. XPS spectra were acquired with a Kratos AXIS ULTRA spectrometer with a monochromated Al $K\alpha$ source ($h\nu = 1486.6$ eV). All spectra were referenced to the main C 1s peak at 284.8 eV to compensate for charging effects.

3. Results

3.1. C_6H_6 on amorphous SiO_2

Initial experiments were performed in which C_6H_6 films adsorbed directly on the SiO_2 surface were irradiated with electrons in the energy range 100–350 eV. No clear C_6H_6 ESD signal was detected during these irradiation experiments for any C_6H_6 exposure, indicating that no significant C_6H_6 desorption occurs from this surface. A very small constant desorption signal was sometimes observed and attributed to limited thermal desorption. Similarly, no C_6H_6 desorption was observed in experiments performed with thicker multilayer C_6H_6 films. However, post-irradiation Temperature Programmed Desorption (TPD) measurements (data not shown) revealed a reduced C_6H_6 surface concentration. Reflection–Absorption Infrared Spectroscopy (RAIRS) measurements did not reveal the presence of any reaction products, again indicating only a reduction in the amount of adsorbed C_6H_6. By assuming first order desorption kinetics, a cross-section of *ca.* 5×10^{-17} cm^2 was estimated from the decay in TPD yield as a function of irradiation time.

These observations and the associated cross-section are consistent with previous studies of the 150 eV electron irradiation of both chemisorbed and multilayer C_6H_6 on W (110), in which no C loss during irradiation was observed using a combination of Auger electron spectroscopy (AES) and X-ray photoelectron spectroscopy (XPS) [16]. The dominant process promoted by the low energy electrons was dehydrogenation, resulting in the formation of a carbonaceous layer. Indeed, in our experiments, after multiple irradiation experiments where C_6H_6 films were first adsorbed directly on the SiO_2 substrate, the formation of a deposit on the substrate was visible by eye. The nature of this deposit was investigated with XPS. This required the removal of the substrate from UHV and transport to the University of Nottingham where the analysis was carried out. XP spectra were therefore obtained both for a freshly deposited SiO_2 film, and two which had been used in ESD experiments. Figure 1 compares the C 1s, Si 2p and O 1s peaks for the the fresh SiO_2 and a film used in several ESD experiments. The C 1s peak shows the same structure for all three samples. The overall elemental compositions of the three samples, as obtained using standard XPS sensitivity factors [17] are shown in Table 1. The main peak, fixed at 248.8 eV, can be attributed to sp^2-hybridized graphitic carbon atoms or carbon atoms bound to hydrogen atoms [18]. The peaks to higher binding energy most likely result from carbon atoms bound to oxygen atoms. Given that the samples were exposed to atmosphere between ESD and XPS measurements, some oxidation of adsorbed carbon is unsurprising. The small carbon signal present for the fresh SiO_2 can also be attributed to contaminants adsorbed during the transfer. The XPS spectrum of this sample is dominated by the O 1s peak and the ratio between this and the Si 2p peak is consistent with the stoichiometry of SiO_2, allowing for some additional oxygen associated with oxidized contaminants. The two samples that had been used in ESD experiments show a dramatic increase in the amount of adsorbed C and an associated decrease in Si at the surface, indicating the formation of a thick carbonaceous film. The increased C/O ratio is consistent with oxidation of the thicker carbon deposit during the transfer. This also results in an increase in the FWHM of the O 1s peak. The small shift of 0.6 eV to higher binding energy in the Si 2p is thought to originate from the SiO_2 layer charging differently to the carbonaceous layer. These results therefore indicate that the irradiation of C_6H_6 multilayers and C_6H_6 adsorbed on SiO_2 results in the formation of a stable carbon deposit through dehydrogenation, in agreement with previous studies. Unfortunately the H_2 partial pressure was too high to allow the direct observation of the ejection of hydrogen species during irradiation.

3.2. C_6H_6 on compact ASW

In contrast to the irradiation of C_6H_6 adsorbed on SiO_2, significant C_6H_6 desorption resulted from similar experiments performed with C_6H_6 adsorbed on a thick film of compact ASW. Resulting desorption traces are shown in Figure 2 for a C_6H_6 exposure of 1 L. Our previous thermal desorption measurements [14] indicate that this exposure produces a surface layer dominated by isolated C_6H_6 molecules on the compact ASW surface. For all electron energies in the range 100–350 eV used in these experiments, a single desorption feature appears at at the onset of electron irradiation ($t = 0$) which decays rapidly within a few tens of seconds. The decay time decreases with increasing electron energy, indicating an increase in desorption cross-section. Experiments performed with C_6H_6 exposures of 0.1 and 0.5 L resulted in similar decays with reduced signal intensities. This is consistent with the same desorption mechanism being in operation for a lower initial C_6H_6 surface concentration. Given the sub-monolayer coverage that results from these C_6H_6 exposures, we attribute the observed C_6H_6 desorption to the ejection of C_6H_6 molecules directly bound to H_2O molecules at the surface of the compact ASW film.

When the C_6H_6 exposure is increased so that the formation of C_6H_6 islands occurs on the compact ASW surface [14], a more complex desorption behaviour is observed during irradiation. This is shown in Figure 3, where desorption traces for 10 L of C_6H_6 adsorbed on a thick layer of compact ASW are displayed. The rapid desorption component observed in Figure 2 is again present, but with a decreased intensity. In addition to this component a second, significantly slower, decay in the C_6H_6 desorption signal is ob-

served. It is clear that this decay does not begin immediately at $t = 0$, but at some later time. This is particularly pronounced at higher electron energies where an increase in signal occurs prior to the second decay. The desorption mechanism that leads to this slow desorption component must also involve the underlying compact ASW substrate, given that no C_6H_6 desorption is observed during the irradiation of 10 L of C_6H_6 adsorbed directly on the SiO_2. Experiments performed with thicker C_6H_6 multilayer films adsorbed on top of the compact ASW substrate showed similar desorption behaviour, but with significantly reduced signal intensity, as shown in Figure 4 for a 200 L C_6H_6 film. This is consistent with the behaviour observed for the irradiation of C_6H_6 multilayers.

4. Discussion

Desorption cross-sections were obtained for the single decays shown in Figure 2 by assuming first order desorption kinetics and fitting the initial decay region with single component exponential decay functions of the form [19]:

$$I(t) = I_0 \exp[-\sigma\phi t] + I_\infty \quad (1)$$

where $I(t)$ is the desorption signal intensity, I_0 is the initial intensity at $t = 0$, σ is the desorption cross-section in cm^2 and ϕ is the experimental electron flux in electrons cm^{-2} s^{-1}. The constant background value, I_∞ is included to account for the slight non-zero background at long times. This most likely arises from a small thermal desorption component and has minor impact on the derived cross-sections. The same fitting procedure was also performed for the 10 L C_6H_6 ESD data. The calculated C_6H_6 desorption cross-sections obtained in this way are shown in Figure 5 as a function of incident electron energy. The cross-sections, which are in excess of 10^{-15} cm^2, tend to increase with increasing electron energy and indicate a highly efficient desorption mechanism. This cross-section is significantly larger than those typically measured for the desorption of, for example, species from metal substrates [20]. The cross-sections corresponding to the fast desorption component for the two C_6H_6 film thicknesses are comparable. This indicates that this component results from the same mechanism in both cases. However, it is clear that the intensity of this component is smaller in the case of the 10 L C_6H_6 film. It should be noted that the cross-sections were derived using the incident electron flux and therefore reflect the overall process including the formation of secondary electrons, as will be discussed.

It is clear that a single exponential decay fit is insufficient for the more complex desorption behaviour observed in Figure 3. A second exponential decay function was included to account for the slower desorption component. The peak, which is clearly evident in several of the experimental decays, indicates that there is some delay in the appearance of this second component. The following function, was therefore used to fit the experimental ESD profiles:

$$I(t) = I_1 \exp[-\sigma_1\phi t] + I_2\left(\exp[-\sigma_2\phi t] - \exp\left[-\frac{t}{\tau}\right]\right) + I_\infty \quad (2)$$

with the first term being analogous to the simple decay in Eq. 1. The second term contains the slow desorption component with a desorption cross-section, σ_2, and the associated appearance with a time constant τ. The resulting fits are shown in Figure 3. The cross-sections for the fast component were fixed with the values obtained from the initial decay region shown in Figure 5. This assumption was necessary in order to obtain a unique fit and is reasonable given the similarity of the fast cross-sections obtained for the two film thicknesses. The cross-sections for the slow desorption component were found to be an order of magnitude smaller, with a typical value of $(6 \pm 4) \times 10^{-17}$ cm^2. There is some indication of a slight increase in cross-section with increasing electron energy, but the uncertainties in the fitting preclude any definitive conclusion from being made on the nature of this trend. A mean value of 7 ± 4 s was obtained for the time constant associated with the appearance of this component. This timescale is comparable to that associated with the fast desorption component, which rises from around 2.5 to 7 s over the energy range investigated. This suggests that these features may be related.

It is clear that the desorption of C_6H_6 relies on the presence of the compact ASW substrate. For incident electrons with energies of the order 100 eV the total ionization cross-section is around 10^{-16} cm^2 [21] indicating that further excitations are involved. More detailed investigations will be essential to fully elucidate the desorption mechanism that results in the observed large cross-section. However, the size of this cross-section can to some extent be rationalized by considering that each primary electron

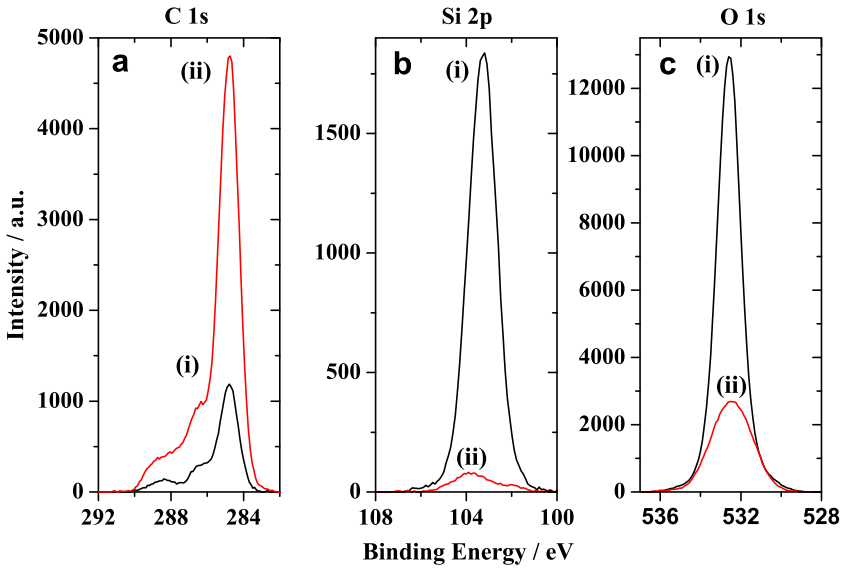

Figure 1. XPS spectra obtained for (i) a fresh SiO_2 film and (ii) a SiO_2 film used in multiple ESD experiments. High resolution spectra for the (a) C 1s, (b) Si 2p, (c) O 1s regions are shown. A clear reduction in the Si and O signals and increase in the C signal results from the ESD experiments.

Table 1
Elemental composition of the fresh SiO_2 film and the deposit formed after multiple ESD experiments.

	%C	%O	%Si
Fresh SiO_2	17	59	24
Deposit 1	76	22	2
Deposit 2	77	20	3

can result in multiple excitation events during its passage through the compact ASW film, along with the formation of secondary electrons. For example, calculations have shown that 450–500 eV Auger electrons will produce around 25 secondary electron within ice [22], each of which could contribute to the observed cross-section. As noted previously, the cross-sections reported in the present study were derived using the incident electron flux. These values therefore represent the overall efficiency of the desorption process with respect to the incident electron beam. This represents a combination of both direct desorption promoted by the incident electron beam and that resulting from secondary electrons formed in the ice. It should be noted that the cross-section derived from the overall electron flux, taking account of the secondary electrons involved, may be up to an order of magnitude smaller considering a secondary electron yield of the order of 10. However, from an astrophysical viewpoint, for example, it is important to appreciate the efficiency of the overall desorption process resulting from the incident beam.

It is worth noting that C_6H_6 is known to form weak hydrogen bonds with H_2O [23]. This will effectively result in a $C_6H_6{-}(H_2O)_n$ cluster structure for an isolated C_6H_6 molecule adsorbed on a H_2O surface. The dissociation energy for the $C_6H_6{-}H_2O$ cluster has been measured to be 0.098 eV [24], compared to the $H_2O{-}H_2O$ dissociation energy of 0.15 eV [25]. Mechanisms that can result in the desorption of H_2O molecules and/or fragments and ions from the compact ASW surface are also likely to result in the ejection of these C_6H_6 molecules. Although not investigated in detail, H_2O desorption was observed in the present study. Given the cascade of secondary electrons produced, it is likely that several processes lead to the observed C_6H_6 desorption. The range of possible excitations is highlighted by the rich photon absorption spectrum of amorphous ice [26] wich has a threshold around 7.5 eV. Previous investigations have demonstrated the desorption of energetic protons with kinetic energies of several eV from the surface region [27,28] as a result of a range of excitations in the energy range 21–70 eV. Low energy DEA to H_2O molecules has been shown to result in anion desorption, although for amorphous ice the ion yield was found to be significantly reduced for thick films [4,29]. As well as direct excitation, ionization followed by electron–ion recombination has been demonstrated to result in the formation of excitons [30]. Investigations of the D_2 yield, which increased strongly with ASW thickness, indicated that whilst reactions forming D_2 occur at the interface regions, exciton formation occurs within the bulk film. Exciton migration then results in the transfer of energy over lengths of the order of 100 layers to the interface regions. In a subsequent study [8], the desorption of intact D_2O from the vacuum interface was shown to increase with film thickness, indicating that excitations within the bulk of the ice are responsible for processes at the interfaces. The desorption of weakly bound H_2O molecules from the vacuum interface region has also been observed during photon irradiation, where the migration to the surface region of excitons formed within the bulk ice was also implicated [31]. Given the electron energies in the present work, electron penetration into the bulk will occur and it is possible that this energy transfer mechanism plays a role in the desorption of C_6H_6 molecules. We hope to conduct measurements investigating the dependence of the C_6H_6 yield on the thickness of the underlying compact ASW to determine the role played by bulk excitations. It should be mentioned that a cross-sec-

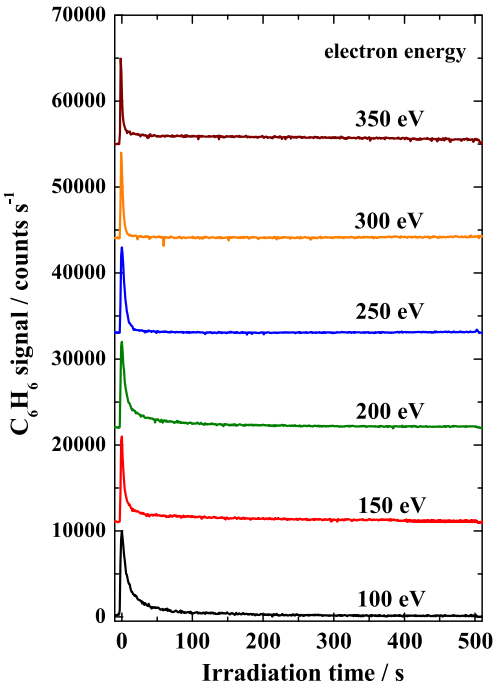

Figure 2. C_6H_6 ESD traces for 1 L of C_6H_6 adsorbed on a thick film of ASW. A single rapid desorption component with a cross-section of the order of 10^{-15} cm^2 is observed. This feature can be attributed to the desorption of isolated C_6H_6 molecules from the compact ASW surface.

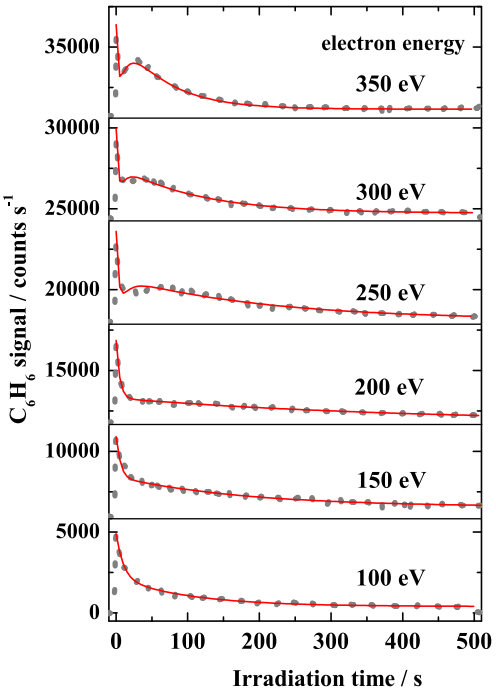

Figure 3. C_6H_6 ESD traces for 10 L of C_6H_6 adsorbed on a thick film of compact ASW (dotted lines). The intensity of the rapid desorption component is reduced as a result of the reduction in the concentration of isolated C_6H_6 molecules. A second decay feature with an associated cross-section of *ca.* 10^{-16} cm^2 is present. This feature can be attributed to the desorption of C_6H_6 molecules diffusing between larger C_6H_6 islands on the compact ASW surface. The solid lines are fits to the experimental data as described in the text.

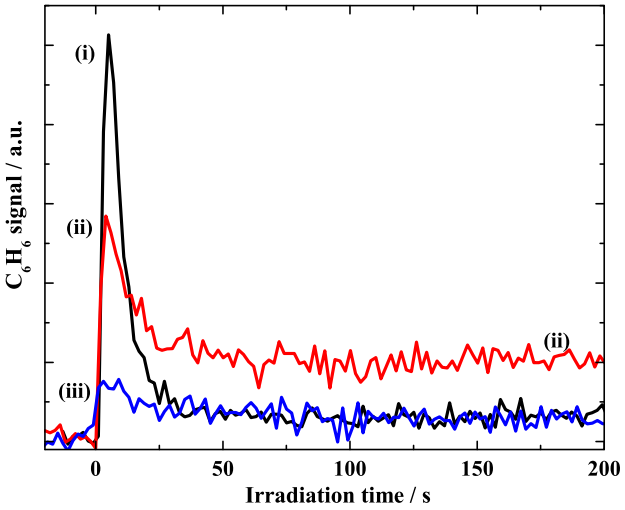

Figure 4. C_6H_6 ESD traces for (i) 5, (ii) 50 and (iii) 200 L of C_6H_6 adsorbed on a thick film of compact ASW an electron energy of 300 eV was used all cases. The desorption signal for 200 L is clearly significantly reduced compared to the low coverage experiments. This highlights the role played by the compact ASW film in the desorption of C_6H_6 molecules.

tion of 5×10^{-16} cm^2 has been measured for the ESD of O_2 from physisorption states on Ag (110) [32], although it is necessary to appreciate the role played by the metal substrate in this case. The large cross-section measured in the present study is particularly surprising given the lack of C_6H_6 desorption in the absence of the compact ASW film.

The mechanism behind the slower decay remains unclear, although the observations indicate that the compact ASW film is again involved. This component dominates the desorption for C_6H_6 film thicknesses where the surface consists of C_6H_6 islands adsorbed on the compact ASW surface. We therefore suggest that diffusion from larger C_6H_6 islands on the surface repopulates the isolated C_6H_6 molecule sites. Experiments in which the electron beam was turned off following the initial decay showed minimal recovery of the fast component upon later irradiation, indicating that any surface diffusion is non-thermal. Diffusion may be promoted by the same exciton-driven mechanism proposed for desorption of isolated C_6H_6 molecules, resulting in the production

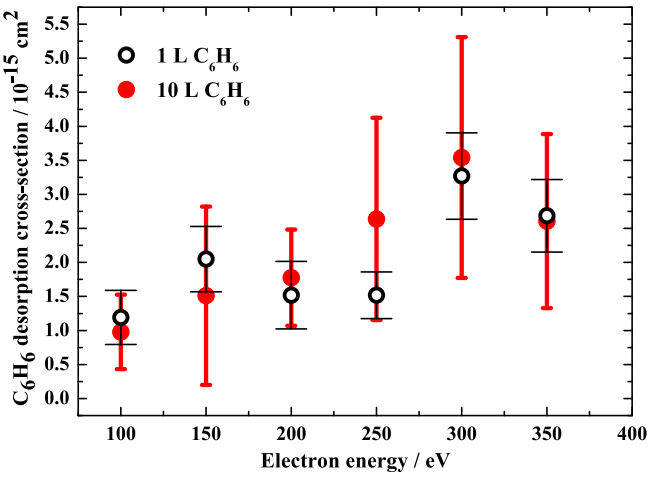

Figure 5. The electron energy dependence of the C_6H_6 desorption cross-section associated with the rapid desorption feature. Data are shown both for a 1 L (open circles, wide error bars) and 10 L (full circles, narrow error bars) C_6H_6 film adsorbed on top of a thick compact ASW film.

of mobile C_6H_6 from the edges of islands which are subsequently desorbed. This would be consistent with the observed correlation between the time constants for the fast desorption component and the growth of this second component. Such a mechanism is somewhat reminiscent of the formation of hot atoms during the photolysis of molecular species adsorbed on metal surfaces, which go on to initiate both chemical and physical processes [33,34]. The slow desorption signal would then represent the net diffusion rate. Further experiments performed at low temperature will be necessary to fully elucidate the nature of this desorption mechanism and how the associated kinetics relate to the detailed structure of the adsorbed film.

Whilst, as noted previously, it was not possible to investigate the desorption of ionic species such as $C_6H_6^+$, it is thought that this is not a dominant channel, at least for the slow desorption signal. In this case, the total loss cross-section was estimated from RAIRS measurements to be around 5×10^{-17} cm^2. This is comparable to that obtained through the ESD measurements, suggesting that $C_6H_6^+$ desorption is limited. We hope to perform measurements investigating the desorption of ions in the future following the required modifications to our experiment.

5. Conclusions

In summary, we report the highly efficient desorption of isolated C_6H_6 molecules from the surface of a compact amorphous solid water film irradiated with electrons in the range 100–350 eV. The observed desorption cross-section, which is in excess of 10^{-15} cm^2, is likely to involve a range of excitations in the underlying compact ASW film. As well as those occuring at the interface region, efficient desorption may be promoted by the formation of excitons within the underlying compact ASW film which migrate to the surface region and lead to the desorption of adsorbed C_6H_6 molecules. A slower desorption component is tentatively attributed to a diffusion-limited desorption mechanism, again promoted by the migration of excitons to the surface region. Further studies are required to investigate in more detail the complicated desorption kinetics of this system.

Acknowledgments

JDT and MPC acknowledge the support of the UK Engineering and Physical Sciences Research Council (EPSRC). The authors thank Dr. Ignacio J. Villar-Garcia for performing the XPS measurements at the University of Nottingham Nanotechnology and Nanoscience Centre. These were performed under the EPSRC Free and Open-access Materials Analysis Scheme. Financial support from Heriot-Watt University for a number of upgrades to the UHV system is also acknowledged. Astrochemistry research at Heriot-Watt and Aarhus Universities is part of the LASSIE-ITN network, which is supported by the European Commission's 7th Framework Programme under Grant Agreement Number 238258.

References

[1] C.J. Bennett, C.S. Jamieson, Y. Osamura, R.I. Kaiser, Astrophys. J. 653 (2006) 792.
[2] S. Yamamoto, A. Beniya, K. Mukai, Y. Yamashita, J. Yoshinobu, Chem. Phys. Lett. 388 (2004) 384.
[3] A.D. Bass, L. Sanche, Low. Temp. Phys. 29 (2003) 202.
[4] P. Rowntree, L. Parenteau, L. Sanche, J. Chem. Phys. 94 (1991) 8570.
[5] G.A. Kimmel, T.M. Orlando, C. Vezina, L. Sanche, J. Chem. Phys. 101 (1994) 3282.
[6] T.M. Orlando, G.A. Kimmel, Surf. Sci. 390 (1997) 79.
[7] N.G. Petrik, A.G. Kavetsky, G.A. Kimmel, J. Chem. Phys. 125 (2006) 124702.
[8] N.G. Petrik, G.A. Kimmel, J. Chem. Phys. 123 (2005) 054702.
[9] G.A. Grieves, T.M. Orlando, Surf. Sci. 593 (2005) 180.
[10] W. Zheng, D. Jewitt, R.I. Kaiser, Astrophys. J. 639 (2006) 534.
[11] D.J. Oakes, M.R.S. McCoustra, M.A. Chesters, Discuss. Faraday Soc. 96 (1993) 325.

[12] J.D. Thrower, M.P. Collings, F.J.M. Rutten, M.R.S. McCoustra, Mon. Not. R. Astron. Soc. 394 (2009) 1510.
[13] G.A. Kimmel, K.P. Stevenson, Z. Dohnlek, R.S. Smith, B.D. Kay, J. Chem. Phys. 114 (2001) 5284.
[14] J.D. Thrower, M.P. Collings, F.J.M. Rutten, M.R.S. McCoustra, J. Chem. Phys. 131 (2009) 244711.
[15] T.M. Orlando, M.T. Sieger, Surf. Sci. 528 (2003) 1.
[16] J.E. Whitten, R. Gomer, Surf. Sci. 347 (1996) 280.
[17] D. Briggs, M.P. Seah (Eds.), Practical Surface Analysis, vol. 1, Wiley, Chichester, UK., 1990.
[18] H. Ago, T. Kugler, F. Cacialli, W.R. Salaneck, M.S.P. Shaffer, A.H. Windle, R.H. Friend, J. Phys. Chem. B103 (1999) 8116.
[19] S.W. Bellard, E.M. Williams, Surf. Sci. 80 (1979) 450.
[20] T.E. Madey, J.T. Yates, J. Vac. Sci. Technol. 8 (1971) 525.
[21] M. Vinodkumar, K.N. Joshipura, C.G. Limbachiya, B.K. Antony, Nucl. Instrum. Methods Phys. Res. B 212 (2003) 63.
[22] N. Timneanu, C. Caleman, J. Hajdu, D. van der Spoel, Chem. Phys. 299 (2004) 277.
[23] S. Suzuki, P.G. Green, R.E. Bumgarner, S. Dasgupta, I. Goddard, A. William, G.A. Blake, Science 257 (1992) 942.
[24] B.M. Cheng, J.R. Grover, E.A. Walters, Chem. Phys. Lett. 232 (1995) 364.
[25] M.W. Feyereisen, D. Feller, D.A. Dixon, J. Phys. Chem. 100 (1996) 2993.
[26] K. Kobayashi, J. Phys. Chem. 87 (1983) 4317.
[27] R.H. Stulen, P.A. Thiel, Surf. Sci. 157 (1985) 99.
[28] M.T. Sieger, W.C. Simpson, T.M. Orlando, Phys. Rev. B 56 (1997) 4925.
[29] W.C. Simpson, T.M. Orlando, L. Parenteau, K. Nagesha, L. Sanche, J. Chem. Phys. 108 (1998) 5027.
[30] N.G. Petrik, G.A. Kimmel, Phys. Rev. Lett. 90 (2003) 166102.
[31] J. Bergeld, D. Chakarov, J. Chem. Phys. 125 (2006) 141103.
[32] I. Rzeznicka, J. Lee, J.T. Yates, J. Phys. Chem. C 111 (2007) 3705.
[33] W. Ho, Surf. Sci. 299 (1994) 996.
[34] A.N. Artsyukhovich, I. Harrison, Surf. Sci. 350 (1996) L199.